Keto-enol tautomerization of 2-(2′-hydroxyphenyl)benzoxazole and 2-(2′-hydroxy-4′-methylphenyl)benzoxazole in the triplet state: Hydrogen tunneling and isotope effects. 1. Transien...

ARTICLE *in* THE JOURNAL OF PHYSICAL CHEMISTRY B · DECEMBER 1991

Impact Factor: 3.3 · DOI: 10.1021/j100178a043

3 AUTHORS, INCLUDING:

Wajih Al-Soufi
University of Santiago de Compostela
74 PUBLICATIONS **741** CITATIONS

fraction efficiency drops to zero. Later, as the new product concentration grating increases even more, α_1 becomes negative. As a consequence, the total diffraction efficiency starts to rise again, $\sinh^2$ being an even function (see eq 1).

Conclusion

Boric acid glass doped with triphenylene is well suited for gated hologram recording at low light intensities of the order of a few mW/cm^2. The measured diffraction efficiencies are small due first to the low concentration of the active compound (10^{-3} M) in the matrix and second to the wavelengths at which the holograms are read. Higher diffraction efficiencies can probably be obtained with higher dopant concentrations and by reading the holograms at a wavelength corresponding to the absorption maximum of the product.

In the present paper, we also showed the importance of the wavelength of the reading beam on the diffraction efficiency. In order to obtain higher holographic efficiency, the magnitude of absorption coefficient and molar refraction of educt and product at the reading wavelength should be as different as possible. Either the absorption coefficient and molar refraction of product should be much larger than those of the educt when the product concentration grating dominates or those of the product should be much smaller that those of the educt when the holographic efficiency results from the educt concentration grating. Intermediate cases, where the magnitudes of product and educt absorption coefficients and molar refraction are similar, lead to a complicated behavior. This does not apply for intermediate states like the triplet state, whose contribution vanishes if this state is not continuously repopulated. On the other hand, such interference between product, educt, and intermediate state gratings can give valuable information on the dynamics and the kinetics of the reacting systems, information which sometimes cannot be obtained through conventional methods.

Acknowledgment. We express our thanks to Dr. F. A. Burkhalter for his invaluable help during the early phases of the experimental work and to Dr. A. Renn and Dr. K. Holliday for helpful discussions. This work was supported by the Swiss National Science Foundation.

Keto–Enol Tautomerization of 2-(2′-Hydroxyphenyl)benzoxazole and 2-(2′-Hydroxy-4′-methylphenyl)benzoxazole in the Triplet State: Hydrogen Tunneling and Isotope Effects. 1. Transient Absorption Kinetics

Wajih Al-Soufi, Karl H. Grellmann,* and Bernhard Nickel

Max-Planck-Institut für Biophysikalische Chemie, Abt. Spektroskopie, Am Fassberg, W-3400 Göttingen, Germany *(Received: August 1, 1991)*

Hydrogen tunnel effects in the metastable triplet states of 2-(2′-hydroxyphenyl)benzoxazole (HBO) and 2-(2′-hydroxy-4′-methylphenyl)benzoxazole (*m*-MeHBO) and their deuteriooxy analogues DBO and *m*-MeDBO have been investigated between 35 and 250 K in three alkane solvents that have drastically different viscosities at low temperatures. In the triplet states of HBO the hydrogen transfer between the enol and keto tautomers is reversible because the two triplet states are isoenergetic. In *m*-MeHBO the hydrogen transfer is virtually unidirectional because the initially populated keto triplet state has a higher energy than the enol triplet state. In spite of these differences the observed hydrogen-transfer rate constants of the two compounds have nearly the same values. The temperature dependence of the rate constants is insensitive to large changes in solvent viscosity, i.e., hydrogen tunneling in HBO and *m*-MeHBO depends on solvent friction neither at intermediate nor at very low temperatures. The couples HBO, DBO and *m*-MeHBO, *m*-MeDBO are the first examples where the determination of tunneling rate constants has been extended for both isotopomers into a temperature region where the rates and the isotope effect on these rates become temperature independent.

I. Introduction

For the study of light-induced hydrogen- or proton-transfer processes 2-(2′-hydroxyphenyl)benzoxazole (HBO) is a very interesting compound because it can exist in two tautomeric forms, the enol tautomer (E) and the keto tautomer (K), whose relative stabilities depend on their electronic state. In the electronic ground state of HBO the enol form, ^{1}E, is the stable tautomer. In its first excited singlet state, ^{1}E*, very rapid adiabatic proton transfer takes place,[1] yielding the first excited singlet state of the keto tautomer, ^{1}K*, whose energy is 2100 cm^{-1} lower[2] than that of ^{1}E*.

^{1}K* is depopulated by thermally activated internal conversion and fluorescence to the keto singlet ground state, ^{1}K, and by intersystem crossing to the keto triplet state, ^{3}K*.[3] The keto tautomer is in its singlet ground state less stable than ^{1}E (energy difference 4900 cm^{-1})[2] and decays therefore rapidly to ^{1}E. The quantum yield of intersystem crossing from ^{1}E* to the enol triplet state, ^{3}E*, is virtually zero because of the ultrafast proton transfer

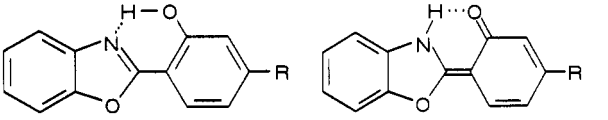

E E_m K K_m

R = H: HBO

$R = CH_3$: m-MeHBO

^{1}E* ⇝ ^{1}K*. This initial population of the *keto* triplet state is a very interesting photophysical property of HBO, because it allows one to study the kinetics of a hydrogen-transfer reaction in the metastable triplet state: We have shown recently[4] that after the formation of ^{3}K*, which takes place within a few nanoseconds, the equilibrium $^3K^* \rightleftharpoons {}^3E^*$ is established between the keto and enol triplet state (Scheme I). Below ~200 K, the rate constants of this reaction are predominantly determined by hydrogen tunnel

(1) Woolfe, G. J.; Melzig, M.; Schneider, S.; Dörr, F. C. *Chem. Phys.* **1983**, *77*, 213 and references therein.
(2) Rodriguez Prieto, M. F.; Nickel, B.; Grellmann, K. H.; Mordziński, A. *Chem. Phys. Lett.* **1988**, *146*, 387.
(3) Mordziński, A.; Grellmann, K. H. *J. Phys. Chem.* **1986**, *90*, 5503.
(4) Grellmann, K. H.; Mordziński, A.; Heinrich, A. *Chem. Phys.* **1989**, *136*, 201.

0022-3654/91/2095-10503$02.50/0

SCHEME I

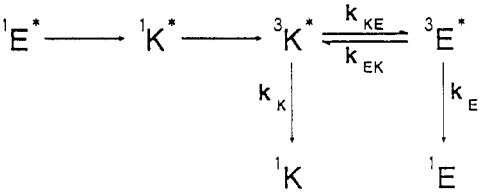

effects. By chance, the two triplet states $^3K^*$ and $^3E^*$ are isoenergetic. Therefore, one observes a *dual* phosphorescence with distinct spectra of the keto phosphorescence $^3K^* \rightarrow {}^1K$ and the enol phosphorescence $^3E^* \rightarrow {}^1E$, whose relative intensities do not change with temperature in fluid solution.[2] As a consequence the rate constants k_K and k_E of the decay processes $^3K^* \rightsquigarrow {}^1K$ and $^3E^* \rightsquigarrow {}^1E$ cannot be determined individually, because they are coupled by the equilibrium $^3K^* \rightleftharpoons {}^3E^*$ and the monoexponential triplet decay yields only the weighted sum θ_2 of the two rate constants, $\theta_2 = \alpha k_K + (1 - \alpha)k_E$ (cf. eq 12). In glassy solutions of HBO the triplet decay is site dependent; from the resulting nonexponential triplet decay the rate constants k_K and k_E can be evaluated.[5]

To complement the evaluation of k_K and k_E and to get more experimental information about the hydrogen tunnel processes governing the establishment of the equilibrium $^3K^* \rightleftharpoons {}^3E^*$, it appeared promising to modify HBO in such a way that the keto triplet state (which is populated initially) lies energetically above the enol triplet state. This has been achieved by a very modest modification of HBO, namely, by introducing a methyl group in meta position to the OH group of HBO, yielding 2-(2′-hydroxy-4′-methylphenyl)benzoxazole (*m*-MeHBO).

In this paper we report the results of a laser flash *absorption* study of HBO and *m*-MeHBO and their deuteriooxy analogues DBO and *m*-MeDBO. In part 2,[6] the *phosphorescence* properties of these compounds are studied and compared.

II. Experimental Section

A. Solvents and Compounds. The solvents cyclopentane (CP), isopentane (=2-methylbutane, IP), 3-methylpentane (3MP), and methylcyclopentane (MCP; all Fluka, purum) were purified chromatographically on a silica–aluminum oxide column immediately before use.[4] Isobutane (IB; Linde, 99.95%, contained in a steel bottle with valve) was used as received.

The mixture isobutane/cyclopentane/methylcyclopentane (2:1:1 by volume; IB-CP-MCP) was prepared[7] by placing a 1:1 mixture (by volume) of CP and MCP in a graduated glass tube with a flange for attachment to a vacuum line. The mixture was cooled to −16 °C under exclusion of moisture in an ice/rock salt bath. Into the known volume of this mixture (measured at −16 °C) isobutane was condensed by slowly bubbling gaseous isobutane through the mixture until its volume had doubled. The cooled tube was attached to the vacuum line, and the solvent mixture was transferred by distillation under vacuum into a liquid nitrogen cooled storage vessel of the flash-cell attachment. If the buffer volume of the flash-cell attachment is large enough, it is not dangerous to handle sealed-off cells around 20 °C. When solutions are to be investigated at very low temperatures, one has to make sure during the cooling procedure, that isobutane recondensing from the vapor phase is thoroughly mixed with the liquid phase, otherwise crystallization may start from the top of the solution.

2-(2′-Hydroxy-4′-methylphenyl)benzoxazole (*m*-MeHBO) was prepared by condensation of 2-hydroxy-4-methylbenzoic acid and 2-(hydroxyamino)phenol at 180 °C. The crude product was purified on a SiO_2 column with diisopropyl ether as eluant; *m*-MeHBO appeared in the first fraction. The yield was very poor (~1%). Recrystallization from cyclohexane yielded colorless needles, mp 145–146 °C (uncorrected). The NMR spectrum is in agreement with the structure of *m*-MeHBO.

The purification of HBO, the degassing and drying of the solutions, and deuteration of the compounds have been recently reported in detail.[4]

B. Flash Apparatus. The laser flash experiments were carried out with an exciplex laser (Lambda Physik, LPX 100; 248 or 308 nm; pulse width ≈10 ns; laser energy ≈50 mJ). The flash cell, the cooling system, and the data analysis have been described.[4] For recording-times $\tau \leq 100$ μs we used a Hamamatsu R928 photomultiplier, a photomultiplier circuit with active components, and a pulsed 150-W Osram XBO-lamp as monitoring light source;[4] for longer recording times a passive photomultiplier circuit with variable load-resistor and a 20-W tungsten–iodine quartz lamp were employed. The position of the two monitoring light sources was fixed; the beam of either light source could be fed through the flash cell with a toroidal mirror which could be flipped into one of two prefixed positions.

III. Kinetic Considerations

Notation. In cases where it is necessary to distinguish between HBO and *m*-MeHBO, the symbols for the electronic states and for the rate constants of *m*-MeHBO will be labeled $^3K_m^*$ and k_K^m. To distinguish between the isotopomers, an "h" is added for the protonated and a "d" for the deuterated compound, e.g., $^3K_{md}^*$, k_K^{md}.

The time dependence of the concentrations of $^3K^*$ and $^3E^*$ in Scheme I is described by the coupled differential equations

$$d[^3K^*]dt = -k_{KE}[^3K^*] - k_K[^3K^*] + k_{EK}[^3E^*] \quad (1)$$

$$d[^3E^*]/dt = -k_{EK}[^3E^*] - k_E[^3E^*] + k_{KE}[^3K^*] \quad (2)$$

The omission of quadratic terms in eqs 1 and 2 implies that triplet–triplet annihilation is neglected as triplet decay process. For excitation with a nanosecond laser pulse at time $t = 0$, the population of $^3K^*$ by intersystem crossing $^1K^* \rightsquigarrow {}^3K^*$ can be considered as instantaneous on a time scale of microseconds. We assume that $^3E^*$ is exclusively populated by proton transfer $^3K^* \rightsquigarrow {}^3E^*$ from the relaxed keto triplet state and thus obtain the boundary conditions:

$$[^3K^*]_{t=0} \equiv [^3K^*]_0 > 0 \qquad [^3E^*]_{t=0} = 0 \quad (3)$$

With eq 3 the solutions of eqs 1 and 2 are

$$[^3K^*] = \{[^3K^*]_0/(\theta_1 - \theta_2)\}\,[(k_{KE} + k_K - \theta_2)\exp(-\theta_1 t) + (\theta_1 - k_{KE} - k_K)\exp(-\theta_2 t)] \quad (4)$$

$$[^3E^*] = \{k_{KE}[^3K^*]_0/(\theta_1 - \theta_2)\}[-\exp(-\theta_1 t) + \exp(-\theta_2 t)] \quad (5)$$

with

$$\theta_{1,2} = \tfrac{1}{2}[(k_{KE} + k_{EK}) + (k_K + k_E) \pm [(k_{KE} + k_{EK})^2 + (k_K - k_E)^2 + 2(k_{KE} - k_{EK})(k_K - k_E)]^{1/2}] \quad (6)$$

In the following it will be convenient to introduce the equilibrium constant K_{eq} of the keto–enol tautomerism in the metastable triplet state and the relative probability α of the population of $^3K^*$ in thermal equilibrium:

$$K_{eq} = k_{KE}/k_{EK} = [[^3E^*]/[^3K^*]]_{eq} = (1 - \alpha)/\alpha \approx \exp(-hc\delta/k_B T) \quad (7)$$

where

$$hc\delta = E(^3E^*) - E(^3K^*) \quad (8)$$

is the energy difference between the enol and keto triplet state and

$$\alpha = \frac{1}{K_{eq} + 1} = \frac{k_{EK}}{k_{KE} + k_{EK}} \quad (9)$$

For the reactions studied here the relation $\theta_1 \gg \theta_2$ holds (cf. section IVA), and therefore one may assume

$$k_{KE} + k_{EK} \gg k_K + k_E \quad (10)$$

By series expansion of the square root in eq 6 and by neglecting

(5) Nickel, B.; Rodríguez Prieto, M. F. *Chem. Phys. Lett.* **1988**, *146*, 393.
(6) Eisenberger, H.; Nickel, B.; Ruth, A. A.; Al-Soufi, W.; Grellmann, K. H.; Novo, M. *J. Phys. Chem.*, following paper in this issue.
(7) Kensy, U. Diplomarbeit, Universität Göttingen, Germany, 1989.

quadratic and higher terms, eq 6 and eqs 4 and 5 simplify to

$$\theta_1 \approx k_{KE} + k_{EK} \quad (11)$$

$$\theta_2 \approx k_K\alpha + k_E(1 - \alpha) \quad (12)$$

$$[^3K^*] \approx [^3K^*]_0[(1 - \alpha)\exp(-\theta_1 t) + \alpha\exp(-\theta_2 t)] \quad (13)$$

$$[^3E^*] \approx [^3K^*]_0(1 - \alpha)[-\exp(-\theta_1 t) + \exp(-\theta_2 t)] \quad (14)$$

In transient-absorption experiments where both, $^3K^*$ and $^3E^*$, absorb at a given monitoring wavelength, the observed absorbance $A(t)$ is the sum

$$A(t) = \epsilon_K[^3K^*]d + \epsilon_E[^3E^*]d \quad (15)$$

where ϵ_K and ϵ_E are the extinction coefficients of $^3K^*$ and $^3E^*$ at the monitoring wavelength and d is the optical path length. With eq 15 and eqs 11–14 one obtains

$$A(t) \approx [^3K^*]_0 d[(\epsilon_K - \epsilon_E)(1 - \alpha)\exp(-\theta_1 t) + [\epsilon_K\alpha + \epsilon_E(1 - \alpha)]\exp(-\theta_2 t)] \quad (16)$$

As already noted in ref 4, it is very difficult to prepare DBO samples with negligible content of HBO. Therefore, one usually observes the sum of two absorbances, $A_s(t) = A_d(t) + A_h(t)$, which decay independently according to eq 16, if triplet energy transfer between the isotopomers can be neglected, i.e., the decay of $A_s(t)$ has to be described with four exponentials. Since, however, $\theta_1^h \gg \theta_1^d$, the exponential containing θ_1^h can be neglected after very short decay times. Therefore, eq 17 was fitted to traces obtained

$$A^d(t) + A^h(t) \approx [^3K_d^*]_0 d[(\epsilon_K - \epsilon_E)(1 - \alpha_d)\exp(-\theta_1^d t) + [\epsilon_K\alpha_d + \epsilon_E(1 - \alpha_d)]\exp(-\theta_2^d t)] + [^3K^*_h]_0\, d[\epsilon_K\alpha_h + \epsilon_E(1 - \alpha_h)]\exp(-\theta_2^h t) \quad (17)$$

with samples that contained a mixture of DBO and HBO, assuming that the extinction coefficients of HBO and DBO are equal. θ_2^h was determined separately with solutions containing HBO only; its value was used as a fixed parameter in the fits of eq 17 to the absorbance traces.

IV. Results

(A) 2-(2′-Hydroxyphenyl)benzoxazole (HBO) and 2-(2′-Deuteriooxyphenyl)benzoxazole (DBO). Since intersystem crossing $^1E^* \rightsquigarrow {}^3E^*$ cannot appreciably compete with the ultrafast proton transfer $^1E^* \rightsquigarrow {}^1K^*$, only the keto state of HBO, $^3K^*$, is populated immediately after flash excitation. The time within which $^3K^*$ is populated is determined by the lifetime of $^1K^*$, which ranges from 200 ps at 293 K to 6 ns below 150 K.[3] The *decay* of $^3K^*$ and $^3E^*$ (effective rate constant θ_2, cf. eq 12) is, on the other hand, much slower than the equilibration reaction (relation 10). Therefore, the effective rate constant θ_1 (cf. eq 11) is in good approximation the sum of the rate constants of hydrogen (or deuterium) transfer during the equilibration.

In Figure 1 four typical transient absorption curves are shown, which are observed after flash excitation of a carefully dried solution of HBO (Figure 1a,b) or DBO/HBO (Figure 1c,d) in an alkane solvent. The instantaneous rise of the absorbance immediately after flash excitation (A_0, cf. Figure 1a) is due to the rapid formation of $^3K^*$, followed by the equilibration to a mixture of $^3K^*$ and $^3E^*$ (A_{eq}, cf. Figure 1a), which decays within milliseconds (Figure 1b,d) to the ground states ^1K and ^1E. At 420 nm the equilibration results in an increase of the absorbance because at that monitoring wavelength the extinction coefficient of $^3E^*$ is larger than that of $^3K^*$. To determine θ_1^h, eq 16 was fitted to traces like those shown in Figure 1a,b.

In DBO the equilibration (rate constant θ_1^d) is much slower than in HBO (cf. Figure 1a,c). At 100 K, for instance, this isotope effect $\Gamma_1(T) = \theta_1^h/\theta_1^d$ amounts to $\Gamma_1(100\text{ K}) = 700$ (cf. Figure 6). The (equilibrium-coupled) *decay* (rate constant θ_2^d) of the two triplet states $^3K_d^*$ and $^3E_d^*$ is much less affected by this isotopic substitution (cf. Figure 1b,d). The traces in Figure 1c,d were obtained with samples which contained DBO and HBO in the ratio [DBO]:[HBO] ≈ 2:1, and eq 17 was fitted to these traces in order to determine θ_1^d. In the legend of Figure 1 the amplitudes in eq 16 are labeled a_1 and a_2, and in eq 17 a_1^d, a_2^d, and a_2^h.

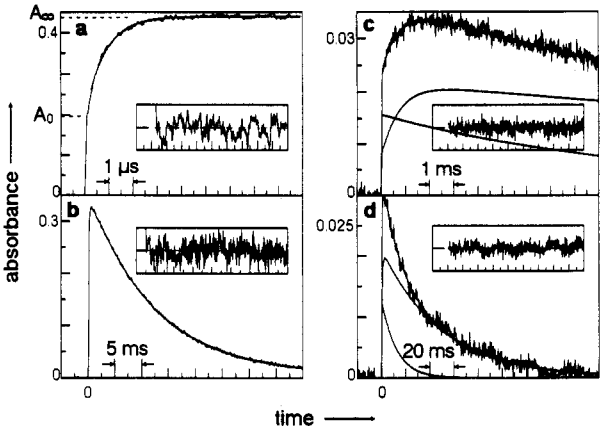

Figure 1. Transient absorptions observed after excitation of a 1×10^{-4} M solution of HBO (a and b) and of DBO/HBO (c and d) in 3MP-IP at 100 K with the 248-nm KrF-line of an exciplex laser. Monitoring wavelength λ = 400 nm, optical path length d = 2 cm. Parameters used to fit eq 16 to traces a and b and eq 17 to c and d (see text): (a) $a_1 = (-2.39 \pm 0.02) \times 10^{-1}$, $a_2 = (4.398 \pm 0.002) \times 10^{-1}$, $\theta_1 = (1.19 \pm 0.01) \times 10^6\ s^{-1}$, $\theta_2 = 82\ s^{-1}$ (fixed); (b) $a_2 = (3.525 \pm 0.004) \times 10^{-2}$, $\theta_2 = 81.9 \pm 0.3\ s^{-1}$; (c) $a_1^d = (-1.40 \pm 0.04) \times 10^{-2}$, $a_2^d = (2.18 \pm 0.06) \times 10^{-2}$, $a_2^h = (1.57 \pm 0.08) \times 10^{-2}$, $\theta_1^d = (1.356 \times 0.074) \times 10^3\ s^{-1}$, $\theta_2^d = 19.9\ s^{-1}$ (fixed), $\theta_2^h = 80\ s^{-1}$ (fixed); (d) $a_1^d = -1.40 \times 10^{-2}$ (fixed), $a_2^d = (2.11 \pm 0.005) \times 10^{-2}$, $a_2^h = (1.26 \pm 0.09) \times 10^{-2}$, $\theta_1^d = 1.356 \times 10^3\ s^{-1}$ (fixed), $\theta_2^d = 19.9 \pm 0.4\ s^{-1}$, $\theta_2^h = 80\ s^{-1}$ (fixed). In c the calculated slow builtup of the DBO equilibrium mixture ($^3E_d^* + {}^3K_d^*$) and the calculated decay of the HBO triplets ($^3E_h^* + {}^3K_h^*$) is shown. The sum of these two traces gives the calculated trace which is superimposed on the experimental curve. The deviation between the calculated and the experimental curve is shown as inset. In d the calculated (slower) decay trace of ($^3E_d^* + {}^3K_d^*$) and the calculated (faster) decay trace of ($^3E_h^* + {}^3K_h^*$) are included.

TABLE I: Approximate Viscosities η/cP of 3-Methylpentane (3MP) and 3-Methylpentane–Isopentane (3MP-IP, 1:1 by Volume at 233 K) at Different Temperatures[8,9]

	η/cP			η/cP	
T/K	3MP	3MP-IP	T/K	3MP	3MP-IP
123	10^2	36	98	10^6	10^4
113	10^3	10^2	93		10^5
103	6×10^4	10^3	92		3×10^5
101	2×10^5	3×10^3	91		5×10^5
100	3×10^5	4×10^3	90		10^6
99	6×10^5	7×10^3			

In Figure 2 the rate constants θ_1^h and θ_1^d are shown in an Arrhenius plot. In an earlier paper[4] we have already published part of these results and pointed out, that hydrogen tunnel effects determine the temperature dependence of these two rate constants. Since it is an important question whether the solvent viscosity has an influence on tunnel effects, we extended our measurements to lower temperatures and determined θ_1 in three different solvents: 3MP, 3MP-IP, and IB-CP-MCP. The viscosities of these solvents[8,9] differ drastically at lower temperatures (cf. Table I). The glass transition temperature of 3MP is ~88 K.[2,5] The viscosity of IB-CP-MCP is not accurately known, but it is always lower than the viscosities of the other two solvents. At 77 K, 3MP forms a very rigid but brittle glass, 3MP-IP is glassy and stable (it cracks at ~55 K) but IB-CP-MCP is still fluid ($10^4 > \eta/\text{cP} > 10^3$) at this temperture (it cracks at ~30 K). The rate constants in Figure 2 are obviously not altered by this drastic variation of solvent viscosity.

(B) 2-(2′-Hydroxy-4′-methylphenyl)benzoxazole (*m*-MeHBO) and 2-(2′-Deuteriooxy-4′-methylphenyl)benzoxazole (*m*-MeDBO). In Figure 3 the absorption and fluorescence spectra of HBO and *m*-MeHBO are shown together for comparison. As one would expect, the methyl substitution in the 4′ position causes only a

(8) Nickel, B.; Lesche, H., unpublished results. The experimental method is described in ref 9.

(9) Lesche, H.; Klemp, D.; Nickel, B. *Z. Phys. Chem.* **1984**, *141*, 239.

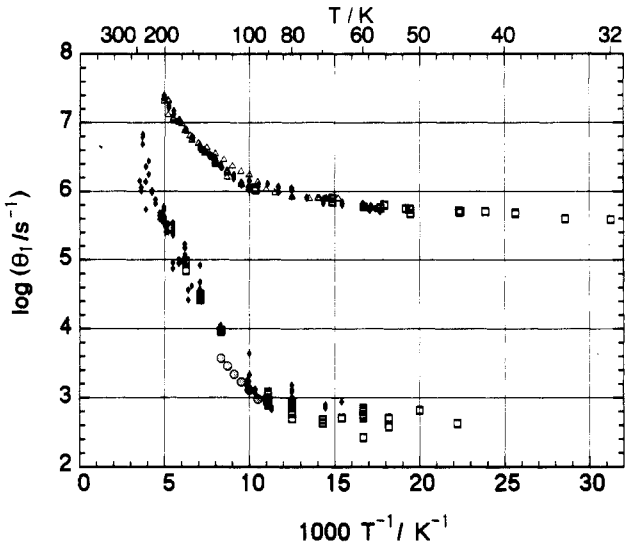

Figure 2. Arrhenius plot of θ_1^h (HBO, upper trace) and of θ_1^d (DBO, lower trace) in three different solvents: 3MP (△), 3MP-IP (◆), IB-CP-MCP (□). For comparison, some phosphorescence data (○, lower trace) from ref 6 are also shown.

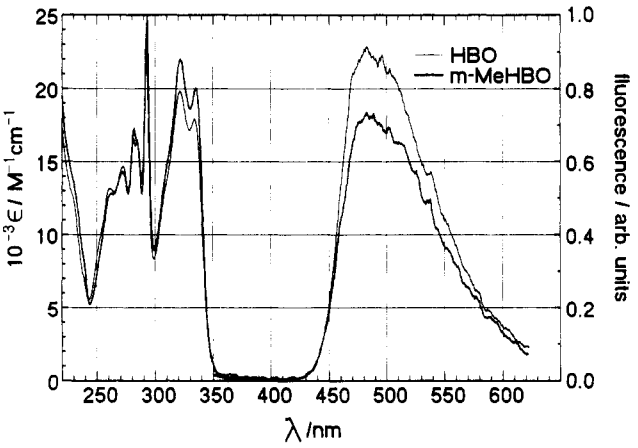

Figure 3. Absorption (left-hand scale) and (uncorrected) fluorescence (right-hand scale) spectra of HBO and *m*-MeHBO in 3MP at 293 K. The solutions were prepared with 0.210 mg of HBO and 0.234 mg of *m*-MeHBO in 10.00 mL of 3MP; the optical path length was d = 0.500 cm.

very modest modification of the absorption and fluorescence spectra. (Substitution in the 3′ or 5′ position (ortho or para to the OH group) causes a 3–8-nm red-shift of the first absorption band and of the fluorescence band.) Since *m*-MeHBO exhibits (like HBO) in inert solvents only a strongly Stokes-shifted fluorescence, the proton transfer in the first excited singlet state of *m*-MeHBO, $^1E_m^* \rightsquigarrow {}^1K_m^*$, must be also very rapid. The fluorescence quantum yield, Φ_f^m, of *m*-MeHBO increases, like that of HBO, with decreasing temperature and becomes constant (Φ_{f0}^m) below 140 K, because the contribution of thermally activated internal conversion to the decay of $^1K^*$ becomes negligible. From the temperature dependence of the relative quantum yields $\Phi_f^m(T)/\Phi_{f0}^m$ we obtain for the activation energy, E_{ic}^m, of this process E_{ic}^m = 18 ± 1 kJ/mol, similar to HBO, where E_{ic} = 15 ± 1 kJ/mol.[3] Obviously, the photophysical properties of *m*-MeHBO are in the singlet manifold very similar to those of HBO. For this reason it is not surprising that the transient absorption signals observed with *m*-MeHBO in nanosecond flash experiments are also quite similar to those obtained with HBO (cf. Figure 1). From their kinetic analysis we determined θ_1^{mh} for *m*-MeHBO and θ_1^{md} for *m*-MeDBO in the two solvents 3MP and IB-CP-MCP. In Figure 4 Arrhenius plots of the two rate constants are shown.

The instantaneous rise of the absorbance at zero time (A_0^m, like in Figure 1a), recorded at different monitoring wavelengths, affords the absorption spectrum of $^3K_m^*$ which is depicted in

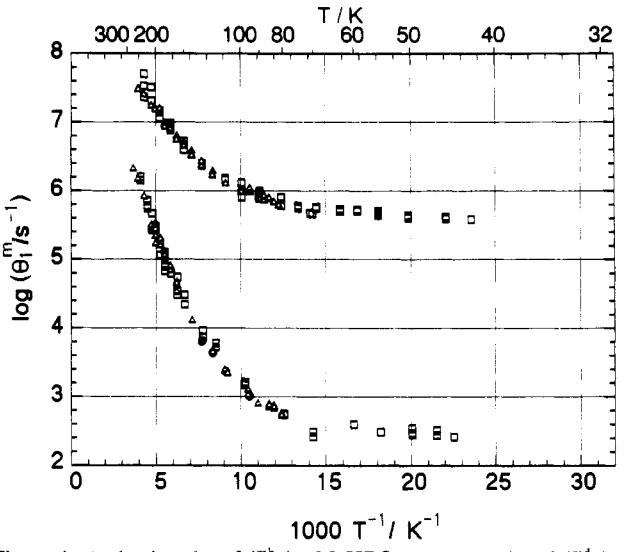

Figure 4. Arrhenius plot of θ_1^{mh} (*m*-MeHBO, upper trace) and θ_1^{md} (*m*-MeDBO, lower trace) in two different solvents: 3MP (△) and IB-CP-MCP (□). For comparison, some phosphorescence data (●, lower trace) from ref 6 are also shown.

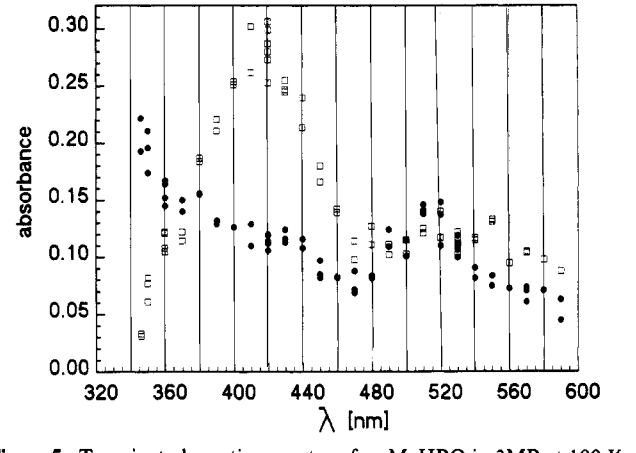

Figure 5. Transient absorption spectra of *m*-MeHBO in 3MP at 100 K obtained from curves similar to those shown in Figure 1a. The A_0 values (●) afford the $^3K_m^*$ spectrum, the A_∞ values (□) the $^3E_m^*$ spectrum (see text).

Figure 5. After equilibration the absorbance (A_{eq}^m, like in Figure 1a) is due to a mixture of $^3K_m^*$ and $^3E_m^*$. In contrast to HBO, where the two triplet states are isoenergetic ($\delta \approx 0$, cf. eq 8), the energy $E(^3K_m^*)$ of the keto triplet state is higher than the energy $E(^3E_m^*)$ of the enol triplet state ($-\delta_m \geq 330$ cm^{-1}), as we will show in part 2.[6] Therefore, the equilibrium constant K_{eq}^m will be shifted to higher values at lower temperatures. A lower bound of $-\delta_m \geq 250$ cm^{-1} can be estimated from absorption measurements as follows: The absorbances before (A_0) and after (A_{eq}) equilibration are given by

$$A_0^m = \epsilon_K[^3K_m^*]_0 d \tag{18}$$

$$A_{eq}^m = \epsilon_K[^3K_m^*]_{eq} d + \epsilon_E[^3E_m^*]_{eq} d \tag{19}$$

where ϵ_K and ϵ_E are the extinction coefficients of $^3K_m^*$ and $^3E_m^*$ at a given monitoring wavelength, λ; d is the optical pathlength. With eq 7 and the boundary condition $[[^3K_m^*] + [^3E_m^*]]_{eq} = [^3K_m^*]_0$ we obtain the ratio

$$F(T) = A_{eq}^m/A_0^m = (1 + K_{eq}^m(T)\epsilon_E/\epsilon_K)/(1 + K_{eq}^m(T)) \tag{20}$$

With increasing temperature K_{eq}^m becomes smaller and $F(T)$ should decrease if $\epsilon_E/\epsilon_K > 1$ (e.g., at λ = 410 nm, cf. Figure 5) and increase, if $\epsilon_E/\epsilon_K < 1$ (e.g., at λ = 350 nm).

The temperature dependence of $F(T)$ has been investigated at temperatures $T \leq 200$ K. Above 200 K the results are not reliable because the triplet yield becomes too small due to the thermally

TABLE II: Triplet Decay Rate Constants of *m*-MeHBO ($\theta_2^{mh} \approx k_E^{mh}$) and *m*-MeDBO ($\theta_2^{md} \approx k_E^{md}$) in 3MP and IB-CP-MCP at Different Temperatures

T/K	solvent	k_E^{mh}/s^{-1}	k_E^{md}/s^{-1}
95	3MP	5.5 ± 0.5	
90		5.2 ± 0.5	1.0 ± 0.1
84		4.3 ± 0.5	1.0 ± 0.1
80		3.0 ± 0.5	0.9 ± 0.2
80	IB-CP-MCP		1.0 ± 0.2
70		3.5 ± 0.5	0.9 ± 0.2
47			0.9 ± 0.2

activated internal conversion of $^1K_m^*$. Between 70 and 200 K we could *not* detect a significant increase (at λ = 350 nm, ϵ_E/ϵ_K = 0.14) or decrease (at λ = 410 nm, ϵ_E/ϵ_K = 2.30) of $F(T)$ with increasing temperature. If $-\delta_m$ were $\leq$250 cm^{-1}, the change of $F(T)$ between 70 and 200 K would be detectable under our experimental conditions. Obviously, $F(T)$ is constant within experimental error because $-\delta_m$ is so large that between 70 and 200 K the equilibrium constant K_{eq}^m is $\gg$1 and, consequently, $F(T) = \epsilon_K/\epsilon_E$ = constant. We conclude that $-\delta_m$ = 250 cm^{-1} gives a lower limit for the energy difference between $^3E_m^*$ and $^3K_m^*$. A higher and more accurate value ($-\delta_m \geq$ 330 cm^{-1}) has been derived from *phosphorescence* data on *m*-MeHBO.[6] If $-\delta_m$ = 330 cm^{-1}, one obtains for the equilibrium constant at 100 K (eq 7) K_{eq}^m(100 K) $\approx$ 112, i.e., in the case of *m*-MeHBO the relative probability α_m of the population of $^3K_m^*$ is $\ll$1 and the absorbance A_{eq}^m is at that temperature almost entirely due to $^3E_m^*$. The open symbols in Figure 5, which are A_{eq}^m values recorded at different monitoring wavelengths, represent therefore the enol triplet–triplet absorption spectrum.

If α_m is $\ll$1, the effective triplet *decay* rate constant (eq 12) becomes for *m*-MeHBO $\theta_2^m \approx k_E^m$, in contrast to HBO where $\theta_2 \approx {}^1/_2(k_K + k_E)$ because in fluid solution $\delta \approx 0$ and, therefore, $\alpha \approx 0.5$. In glassy solution δ becomes site dependent ($\Delta\delta \approx$ 150 cm^{-1}), causing a *nonexponential* triplet-state decay in HBO.[5] From the nonexponential phosphorescence decay in glassy solutions it has been estimated[5] that k_K^h = 206 ± 55 s^{-1} and k_E^h = 5.3 ± 2.0 s^{-1}. The nonradiative decay $^3K^* \rightsquigarrow {}^1K$ is much faster than the nonradiative decay $^3E^* \rightsquigarrow {}^1E$, which is in accord with the energy gap between $^3K^*$ and ^1K (17 500 cm^{-1}) being considerably smaller than the energy gap between $^3E^*$ and ^1E (22 400 cm^{-1}).[2] In very good agreement with the estimate of k_E^h are the directly measured *m*-MeHBO values of k_E^{mh} (cf. Table II). (It is justified to compare k_E^h with k_E^{mh} because the introduction of a 4′-methyl group into HBO can have only a minute influence on the enol triplet decay.) In contrast to HBO, the triplet-state decay of *m*-MeHBO is monoexponential not only in fluid but also in rigid solutions (cf. Table II). We presume that the site-dependent fluctuation of δ_m in *m*-MeHBO is about the same as in HBO ($\Delta\delta_m \approx \Delta\delta \approx$ 150 cm^{-1}). Since, however, $|\delta_m| \geq$ 330 cm^{-1} is much larger than $\delta \approx 0$, this fluctuation has much less influence on α_m than on α, i.e., the relation $\theta_2^m \approx k_E^m$ remains valid for each site. The remarkably large isotope effect on the decay rate constant k_E^m is discussed in part 2.

V. Discussion

The assignment of the transient absorption of solutions of HBO (cf. Figure 1) and *m*-MeHBO to the triplet–triplet absorption of these compounds is unambiguous because it is completely consistent with the phosphorescence data in part 2. In Figures 2 and 4 some of the phosphorescence data are included in the Arrhenius plots of the deuterated compounds to show the good agreement between the results of the two very different experimental methods. In addition, the phosphorescence data show that the population of the enol triplet states of DBO and *m*-MeDBO occurs entirely or, at least, predominantly (≥95%) from the keto triplet states. Thus, the postulation of Scheme I rests on firm grounds.

The most interesting aspect of Scheme I is the establishment of the equilibrium $^3K^* \rightleftharpoons {}^3E^*$, which starts from the initially populated keto triplet state, i.e., *far from equilibrium*. The two couples HBO, DBO and *m*-MeHBO, *m*-MeDBO differ in their kinetic properties in one important aspect: In the case HBO, DBO the two triplet states are isoenergetic ($\delta \approx 0$), i.e., the equilibrium constant $K_{eq} \approx 1$ (eq 7) above the glass transition temperature of the solvent employed. Hence, θ_1 is the effective rate constant of a bidirectional hydrogen transfer during which N–H bonds and O–H bonds are broken and formed (cf. eq 11).

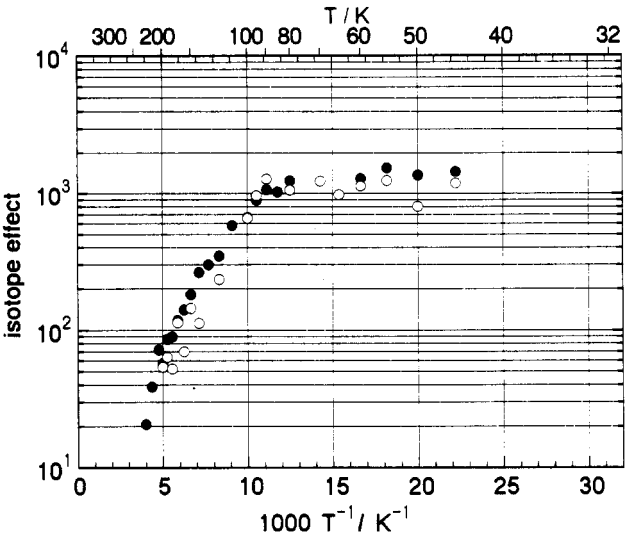

Figure 6. Isotope effects $\Gamma_1 = \theta_1^h/\theta_1^d$ (○) and $\Gamma_1^m = \theta_1^{mh}/\theta_1^{md}$ (●). The points are averaged θ_1 values taken from the data shown in Figure 7.

In *m*-MeHBO, *m*-MeDBO the initially populated keto triplet state has a higher energy than the enol triplet state ($|\delta_m| \geq$ 330 cm^{-1}) and at lower temperatures ($T \leq$ 150 K) K_{eq}^m becomes $\gg$1. Therefore, the equilibration is in this case a virtually unidirectional hydrogen-transfer process where an N–H bond is broken and an O–H bond is formed. In other words, the contribution of k_{EK}^m to the effective rate constant θ_1^m can be neglected, i.e.

$$\theta_1^m \approx k_{KE}^m \tag{21}$$

The difference in the position of the equilibria manifests itself in a most obvious way by the observation that *after* the equilibration of the triplet states in HBO, DBO a *dual* phosphorescence with a time-independent intensity ratio is observed, whereas with *m*-MeHBO, *m*-MeDBO only the phosphorescence from the *enol* triplet state is detectable (cf. part 2). (*During* the equilibration, the phosphorescence from $^3K_{md}^*$ is readily detectable!)

From the temperature dependence of the effective-rate-constant pairs θ_1^h, θ_1^d and θ_1^{mh}, θ_1^{md} (cf. Figures 2 and 4) it is quite obvious that tunnel effects contribute significantly to the hydrogen-transfer rates because[20] the Arrhenius plots in Figures 2 and 4 are not linear and the isotope effects $\Gamma_1 = \theta_1^h/\theta_1^d$ and $\Gamma_1^m = \theta_1^{mh}/\theta_1^{md}$ are large. Figure 6 shows the magnitude and the temperature dependence of the isotope effects.

(10) Yakimchenko, O.; Lebedev, Y. S. *Int. J. Radiat. Phys. Chem.* **1971**, *3*, 17.
(11) Toriyama, K.; Nunome, K.; Iwasaki, M. *J. Am. Chem. Soc.* **1977**, *99*, 5823.
(12) Le Roy, R. J.; Murai, H.; Williams, F. *J. Am. Chem. Soc.* **1980**, *102*, 2325.
(13) Brunton, G.; Gray, J. A.; Griller, D.; Barclay, L. R. C.; Ingold, K. U. *J. Am. Chem. Soc.* **1978**, *100*, 4197.
(14) Limbach, H.; Hennig, J.; Gerritzen, D.; Rumpel, H. *Faraday Discuss. Chem. Soc.* **1982**, *74*, 229.
(15) Prass, B.; Colpa, J. P.; Stehlik, D. *Chem. Phys.* **1989**, *136*, 187.
(16) Grellmann, K. H.; Schmitt, U.; Weller, H. *Chem. Phys. Lett.* **1982**, *88*, 40.
(17) Grellmann, K. H.; Weller, H.; Tauer, E. *Chem. Phys. Lett.* **1983**, *95*, 195.
(18) Al-Soufi, W.; Eychmüller, A.; Grellmann, K. H. *J. Phys. Chem.* **1991**, *95*, 2022.
(19) Bartelt, G.; Eychmüller, A.; Grellmann, K. H. *Chem. Phys. Lett.* **1985**, *118*, 568.
(20) Bell, R. P. *The Tunnel Effect in Chemistry*; Chapman and Hall: London, 1980.

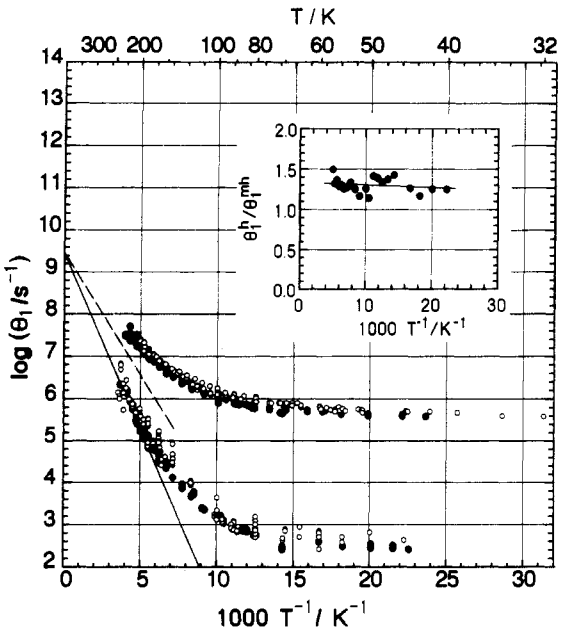

Figure 7. Arrhenius plot of combined data from Figures 2 and 4 without distinction between the solvents. Upper trace: θ_1^h (○) and θ_1^{mh} (●). Lower trace: θ_1^d (○) and θ_1^{md} (●). The inset shows the ratio θ_1^h/θ_1^{mh} from the upper trace.

In spite of the fact that the equilibration is bidirectional in HBO and virtually unidirectional in *m*-MeHBO, the values of the effective rate constants θ_1 and θ_1^m differ only by a small factor which is constant over the entire temperature region covered in Figures 2 and 4. This is shown for the ratio $\theta_1^h/\theta_1^{mh} = 1.3 \pm 0.2$ in the inset of Figure 7 where the data from Figures 2 and 4 are combined without distinction between the solvents.[21]

The strong temperature dependence of the equilibration rate constants at high temperatures in Figure 7 indicates that the hydrogen transfer in the triplet state has a much higher activation energy than in the excited singlet state. Toward lower temperatures the rate constants approach very smoothly a region where they become temperature independent. This smooth transition seems to be a general rule, as far as one can judge from the few reactions where hydrogen tunnel effects could be investigated over a wide temperature range.[4,10-19] Below ~70 K the rate constants become, within experimental error, temperature independent. HBO and *m*-MeHBO are the first examples where this range of thermally nonactivated tunneling could be explored with *both* isotopomers. So far, a few ground-state *hydrogen* tunneling reactions could be investigated[10-19] down to temperatures where the rates became temperature independent, with rate constants typically of the order of 10^{-3} s^{-1}. The deuterium isotope effects on these reactions are quite large, making the determination of the corresponding deuterium-transfer rate constants extremely difficult. The hydrogen- and deuterium-transfer reactions in the triplet states of HBO and *m*-MeHBO have rates in a time range which is experimentally easily accessible. It should therefore be possible to study both rates at still lower temperatures. At present, the limiting factor is the cracking of the solvents at low temperatures. Some preliminary experiments with HBO dissolved in poly(methyl methacrylate) indicate, however, that the reaction rates are very similar to those in alkane solvents. This opens the possibility of studying these reactions at liquid helium temperatures.

To discuss the tunnel effects in some more detail, it is useful to identify the temperature region within which the θ_1 data in Figure 7 could possibly be described with a classical activation energy (V_{cl}). At the most, one can extrapolate the θ_1^d and θ_1^{md} values of the *deuterated* compounds between 200 and 290 K to $1/T = 0$ (solid straight line in Figure 7). The slope of this line corresponds to $V_{cl}^d \approx 16$ kJ/mol ≡ 1346 cm^{-1} and its intercept to a frequency factor of 2.5×10^9 s^{-1}. The latter is a rather low value for a hydrogen-transfer reaction whose promoting mode is an X–H bending and/or stretching vibration (X = O or N). Provided this extrapolation of the "high-temperature" θ_1^d values between 200 and 290 K is justified at all, it yields a *lower* limit of V_{cl}^d and implies that above ~150 K the deuterium transfer occurs predominantly "over the top" of a barrier whose shape were to be defined by some model. For an estimate of the isotope effect on this classical activation energy one may assume $V_{cl}^h \approx 2^{-1/2} V_{cl}^d$ (dashed line in Figure 7). The deviations of the experimental points from this line infer that the θ_1^h and θ_1^{mh} values are determined by tunnel effects over the entire temperature region. For the estimation of an *upper* limit of V_{cl} we assumed in ref 4 a frequency factor of 10^{13} s^{-1} (which is perhaps a more plausible value for a unimolecular reaction) and extrapolated the experimental values to this point under the assumption that the Arrhenius plot becomes linear only at very high temperatures above ~500 K. This extrapolation yielded an estimated barrier height of $V_{cl} \approx 38$ kJ/mol ≡ 3196 cm^{-1} and in that case the θ_1^h, θ_1^{md} *and* the θ_1^d, θ_1^{md} values are entirely determined by tunnel effects.

In any case it follows from both estimates that in the intermediate temperature range the temperature dependence of the hydrogen- and deuterium-transfer rate constants is with certainty caused by thermally activated tunneling. To describe the smooth transition to the region of temperature-independent tunneling, one is forced to assume that not only are high-frequency bending and stretching modes active but also low-frequency modes in the range 100–300 cm^{-1}. If such low-frequency modes are not included in the model, quantum mechanically calculated rate constants become temperature independent at much higher temperatures and much more abruptly than experimentally observed. Presumably, these low-frequency modes result from certain intramolecular vibrations. In two different models[22-25] such low-frequency modes are handled either as an additional degree of freedom leading to a *multidimensional* potential surface (Goldanski et al.[22] and Siebrand et al.[24]) or as a parametric modulation of a *one-dimensional* adiabatic potential (Borgis et al.[24] and Suárez and Silbey[25]). The rate constants are in both approaches calculated by using the golden rule of time-dependent perturbation theory, which requires that the level density in the final state is high to make the transfer irreversible. This is no problem if the reaction is strongly exothermic. In HBO, where the exothermicity of the transfer is approximately zero ($\delta = 0 \pm 15$ cm^{-1}), this condition is presumably met by a strong coupling to the solvent, which leads in glassy solutions to a site-dependent δ. In ref 5 it has been shown that the nonexponential decay of HBO in glassy solution can be well described by the assumption of a Gaussian distribution of δ values with a distribution width of $\Delta\delta \approx 150$ cm^{-1}. The solute–solvent coupling should become increasingly important in the region of temperature-independent θ_1 where the population of low-frequency intramolecular vibrational levels becomes negligible and where tunneling occurs only from the zero vibrational level of the initial state to a primary product state.

In this respect it is very surprising that the θ_1 and θ_1^m values in Figures 2 and 4 are not at all affected by drastic changes of solvent viscosity. Between 88 and 77 K, for instance, 3MP forms a rigid glass, whereas IB-CP-MCP is still liquid. Obviously, solvent friction does neither influence the intramolecular low-frequency vibrations nor those modes of solute–solvent interaction which promote tunneling.

Equally puzzling is the fact that the θ_1 and θ_1^m values differ only by the small and constant factor $\theta_1/\theta_1^m = 1.3 \pm 0.2$ (see inset in Figure 7), although the energy difference between $^3K_m^*$ and $^3E_m^*$

(21) The ratio θ_1^d/θ_1^{md} cannot be determined with the same accuracy because the kinetic analysis of traces from mixed HBO/DBO solutions is more complicated than the analysis of traces from HBO solutions (cf. parts a and c of Figure 1).

(22) Goldanski, V. I.; Fleurov, V. N.; Trakhtenberg, L. I. *Sov. Sci. Rev. B, Chem.* **1987**, *9*, 59.
(23) Siebrand, W.; Wildman, T. A.; Zgierski, M. Z. *J. Am. Chem. Soc.* **1984**, *106*, 4083, 4089.
(24) Borgis, D. C.; Lee, S.; Hynes, J. T. *Chem. Phys. Lett.* **1989**, *162*, 19.
(25) Suárez, A.; Silbey, R. *J. Chem. Phys.* **1991**, *94*, 4809.

($|\delta_m| \geq 330$ cm^{-1}) is appreciably larger than between ^{3}K* and ^{3}E* ($\delta \approx 0$). We expected that the tunneling rates would be much more sensitive to a switch from a reversible (θ_1, cf. eq 11) to a virtually irreversible (θ_1^m, cf. eq 21) reaction. Thus, the data presented in Figure 7 are a challenging test for quantum mechanical models of hydrogen tunneling in condensed media. Incidentally, as a consequence of the insensitivity of the effective rate constants to chemically as well as site-induced changes of δ the equilibration is always monoexponential, even in very rigid solvents.

It will be of great interest to extend the determination of θ_1 and θ_1^m down to liquid helium temperatures where the hydrogen transfer by tunneling must be coupled with simultaneous phonon emission. We presume that between ~20 and 2 K the effective rate constants become again temperature dependent and that the θ_1 and θ_1^m values differ under these conditions more strongly than above 32 K, the lowest temperature covered so far.

Acknowledgment. This work has been supported by the Deutsche Forschungsgemeinschaft (Sonderforschungsbereich 93 "Photochemie mit Lasern"). We thank Prof. J. Troe, Dr. B. Dick, and Mr. A. A. Ruth for helpful discussions, Dr. E. Tauer for the synthesis of *m*-MeHBO, and Mrs. A. Heinrich for technical assistance.

Registry No. E, 835-64-3; E_m, 39720-17-7; K, 64758-55-0; K_m, 136838-65-8; D_2, 7782-39-0.

Keto–Enol Tautomerization of 2-(2′-Hydroxyphenyl)benzoxazole and 2-(2′-Hydroxy-4′-methylphenyl)benzoxazole in the Triplet State: Hydrogen Tunneling and Isotope Effects. 2. Dual Phosphorescence Kinetics

Heike Eisenberger, Bernhard Nickel,* A. Andreas Ruth, Wajih Al-Soufi, Karl H. Grellmann, and Mercedes Novo†

Max-Planck-Institut für Biophysikalische Chemie, Abteilung Spektroskopie, Am Fassberg, W-3400 Göttingen, Germany *(Received: August 1, 1991)*

In the metastable triplet state of 2-(2′-hydroxyphenyl)benzoxazole (HBO) and its deuteriooxy analogue (DBO), the keto tautomer (K) and the enol tautomer (E) have about the same energy, and a dual phosphorescence, $^3K^* \rightarrow {}^1K$ and $^3E^* \rightarrow {}^1E$, can be observed. From the initial time dependence of the dual phosphorescence from DBO the effective rate constant $\theta_1 \approx k_{KE} + k_{EK}$ of the keto–enol equilibration $^3K^* \rightleftharpoons {}^3E^*$ has been determined. $^3E^*$ of DBO is almost exclusively populated from $^3K^*$. In the dual phosphorescence from DBO the relative intensity of the keto band is smaller than in the dual phosphorescence from HBO; this is attributed to a small isotope effect on the keto–enol equilibrium in the triplet state. In the metastable triplet state of 2-(2′-hydroxy-4′-methylphenyl)benzoxazole (*m*-MeHBO) and its deuteriooxy analogue (*m*-MeDBO) the keto–enol equilibrium is strongly shifted to the side of the enol. No keto phosphorescence from *m*-MeHBO is observed. Due to the slower keto–enol equilibration in *m*-MeDBO, an initial keto phosphorescence from *m*-MeDBO can be observed. The values of θ_1 obtained from the time dependence of the phosphorescence of DBO and *m*-MeDBO agree reasonably well with the values obtained from transient-absorption experiments. The rate constants for the nonradiative decays of $^3K^*$ and $^3E^*$ to the electronic ground state are strongly decreased by deuteration.

I. Introduction

2-(2′-Hydroxyphenyl)benzoxazole (HBO) can exist in two tautomeric forms, in an enol form (E) and in a keto form (K). In the metastable triplet state of HBO, accidentally both tautomers have about the same energy, and therefore a dual phosphorescence[1,2] is observed: the keto phosphorescence $^3K^* \rightarrow {}^1K$ and the enol phosphorescence $^3E^* \rightarrow {}^1E$ (see Figure 1).[3] In this paper we present the results of an investigation of the phosphorescence from the related compounds 2-(2′-deuteriooxyphenyl)benzoxazole (DBO) and 2-(2′-hydroxy-4′-methylphenyl)benzoxazole (*m*-MeHBO)[4] and its deuteriooxy analogue (*m*-MeDBO). The paper is complementary to the preceding paper[5] on the transient absorption of these compounds and is concerned with the following items:

(1) The metastable triplet state of all four compounds is populated nearly exclusively by the reaction sequence $^1E \rightarrow {}^1E^* \rightsquigarrow {}^1K^* \rightsquigarrow {}^3K^* \rightleftharpoons {}^3E^*$. In HBO the keto–enol equilibration $^3K^* \rightleftharpoons {}^3E^*$ (cf. Figure 1) is rapid even at low temperatures,[5-7] and we have not been able to measure the phosphorescence from HBO under conditions where the keto–enol equilibrium is not yet established.[1] In DBO, however, under the same conditions the keto–enol equilibration is much slower[5] and can therefore be studied by measuring the initial time dependence of the dual phosphorescence. Thus the results of the transient-absorption experiments on DBO can be verified by an independent method.

(2) Because of the extremely fast tautomerization $^1E^* \rightsquigarrow {}^1K^*$, the population of the enol triplet state by direct intersystem crossing $^1E^* \rightsquigarrow {}^3E^*$ can be completely neglected.[6,7] In the intersystem crossing from $^1K^*$ to the lowest keto triplet state $^3K^*$, two steps are to be distinguished (see Figure 1): (1) the primary process of intersystem crossing, $^1K^* \rightsquigarrow {}^3K^{**}$, where $^3K^{**}$ denotes the primary unrelaxed keto triplet state; (2) the internal conversion and/or vibrational relaxation $^3K^{**} \rightsquigarrow {}^3K^*$. Accordingly, in principle two contributions to the population of the enol triplet state are possible: a very fast contribution $^3K^{**} \rightsquigarrow$

† On leave from Departamento de Química Física, Facultad de Química, Universidad, Santiago de Compostela, Spain.

(1) Rodríguez Prieto, M. F.; Nickel, B.; Grellmann, K. H.; Mordziński, A. *Chem. Phys. Lett.* **1988**, *146*, 387.
(2) Nickel, B.; Rodríguez Prieto, M. F. *Chem. Phys. Lett.* **1988**, *146*, 393.
(3) All considerations of the keto–enol tautomerism in this paper refer to solutions of HBO and its analogues in alkanes, that is, in aprotic and unpolar solvents. In protic and/or polar solvents, the formation of intermolecular hydrogen bonds and intermolecular proton transfer may drastically change the photophysical behavior of HBO.
(4) In the abbreviation *m*-MeHBO for 2-(2′-hydroxy-4′-methylphenyl)-benzoxazole we refer to the meta position of the methyl group relative to the hydroxy group.
(5) Al-Soufi, W.; Grellmann, K. H.; Nickel, B. *J. Phys. Chem.*, preceding paper in this issue.
(6) Mordziński, A.; Grellmann, K. H. *J. Phys. Chem.* **1986**, *90*, 5503.
(7) Grellmann, K. H.; Mordziński, A.; Heinrich, A. *Chem. Phys.* **1989**, *136*, 201.

0022-3654/91/2095-10509$02.50/0